StethoVest: A simultaneous multichannel wearable system for cardiac acoustic mapping

Christos Sapsanis*, Nathaniel Welsh†, Michael Pozin†, Guillaume Garreau‡, Gaspar Tognetti*,
Hani Bakhshaee¶, Philippe O. Pouliquen*, Rajat Mittal†, William R. Thompson§, Andreas G. Andreou*‖
*Department of Electrical and Computer Engineering, †Department of Mechanical Engineering, Johns Hopkins University,
‡IBM Almaden Research Center, §Department of Pediatrics, Johns Hopkins University School of Medicine,
¶L.E.K. Consulting. Email: ‖andreou@jhu.edu.

***Abstract*—Cardiac acoustic mapping remains a highly unexplored area, likely due in part to a decline in research into heart auscultation over the past several decades. However, because the stethoscope remains an integral part of clinical care, novel approaches to improve the accuracy and scope of auscultation are now being explored. The current work introduces an innovative design for heart acoustic mapping based on a microphone array embedded in a wearable vest. The system incorporates a customized design of a front-end readout channel with discrete components paired with analog to digital converter DAQ modules. The main scope is to provide simultaneous recordings of heart sounds to generate spatiotemporal images. This noninvasive and time efficient technique will assist in the exploration of normal and pathological heart activity propagation patterns, providing new knowledge to the current understanding of the cardiac acousteome.**

***Index Terms*—phonocardiogram, heart auscultation, instrumentation, sensor array, heart sounds, wearable, vest, acoustic mapping.**

I. Introduction

Heart auscultation can be traced back to ancient civilizations such as those in Greece and Egypt. The stethoscope was invented by Laennec in 1816 initiating a hundred and fifty-year golden era of interest in research into the interpretation of heart sounds and murmurs. After that period, a decline in this research occurred simultaneously with the advancement of imaging techniques such as echocardiography, computed tomography, and more recently magnetic resonance imaging. While imaging is now highly accurate for diagnosing anatomic and functional abnormalities, these methods are time consuming, have high usage cost and require trained staff for operation and interpretation. As currently practiced, they are not practical or recommended in most cases for population screening for heart disease. Thus, there is now renewed interest in improving heart auscultation as an efficient and accurate screening method [1].

The heart is a highly complex organ requiring the coordination of electrical and mechanical functions. The blood flow is unidirectional due to four valves, the normal and abnormal functioning of which is associated with distinct acoustic signatures. The first (S_1) and second (S_2) heart sounds are mainly related to closure of the atrioventricular valves, mitral and tricuspid, and the semilunar valves, aortic and pulmonary, respectively. Other sounds, called murmurs, are associated with blood flow across these valves and, also have distinct acoustic properties depending on whether or not anatomic abnormalities are present. All of these heart related acoustic sounds propagate from a specific source in the chest, through a medium at a specific speed, and are modified by a combination of human tissues including bone, muscle and fat. Cardiac acoustic mapping focuses on the spatial information derived from chest surface recordings associated with heart sound source and propagation, which can provide important knowledge about the specific condition of the heart.

Auscultation from multiple locations on the chest is conducted clinically using the traditional stethoscope in a sequential fashion, primarily to ascertain differences in sounds that may help differentiate certain pathological conditions. There were investigations of multisite recording during the late 1970s through the late 1980s. The common characteristic was the sequential phonocardiographic (PCG) recordings, where the PCG signals were post-synchronized based on the ECG alignment. There were multiple preliminary efforts reported on the origin of S_1 generation in healthy subjects [2] and on the peak frequency of S_2 in healthy and unhealthy subjects [3]. The first attempt at cardiac acoustic mapping is described by Okada [4], in which 36 positions were recorded from the chest of healthy and unhealthy subjects. The main finding was confirmation of the two components of S_2, where two acoustic energy peaks were detected. Moreover, the studies of Verberg [5] and Vermarien [6] on healthy subjects showed that the heart valves can be modeled as dipole sound sources of the cardiac acoustic waves.

Following further technological development, there were several previous attempts to capture heart sounds with simultaneous multisite recordings. An illustrative example of the approach from that period can be found in the paper by Cozic et al [7], where the realization of a multichannel acoustic system is presented providing acoustic image display using cubic convolution for interpolation. Moreover, a readout system using an acoustic array to generate 2D acoustic mapping images and model simulations, which are used for source localization, are reported by Kompis et al [8]. A more ambitious attempt involved creation of a 3D image of the lung and heart sounds paired with simulations and recordings from a gelatin phantom similar to the dimensions of the human

This research is supported by NSF through grant IIS-1344772 (Mapping the Cardiac Acousteome: Biosensing and Computational Modeling Applied to Smart Diagnosis and Monitoring of Heart Conditions). Christos Sapsanis is a scholar of the "Alexander S. Onassis" Foundation.

core [9]. Nogata et al [10] used a recording system with 64 sensors to generate a high resolution image for visualizing heart acoustic activity.

The current work reports the implementation of a readout circuit with the capability of simultaneous recording in high sampling rate (up to 100 kSamples/sec). Moreover, the PCG microphones are equipped with a mechanical module that allows auto-adjustment and are housed in a wearable vest, as was conceptually described in [11], to provide a reliable and time efficient recording.

II. Materials and Methods

A detailed description for the full system (the recording setup, the mechanical module, the sensors placement and the software) will be provided in the following subsections.

A. Readout System

The system follows a general concept of readout circuits, which consists of a sensor, a preamplification stage, a filtering stage, a main amplification stage and an analog to digital converter (ADC), as depicted in Fig. 1. The skin surface vibrations caused by the cardiac acoustic signal are translated by the sensor into electrical signal due to charge redistribution based on the piezoelectric effect. The received signal is weak (around 5 mV to 10 mV) and, thus, requires a low noise preamplifier (PA) to provide a low-distorted and amplified version of the signal to the next stage. Afterwards, the DC offset and higher order harmonics are eliminated with the use of a high (HP) and low (LP) pass filter with a cut-off frequency set at 0.05 Hz and 4.5 kHz, respectively. The main stage can provide further amplification of 0 dB (buffer), 6 dB or 13 dB. The implemented printed circuit board (PCB) is shown in Fig. 2 (a). Each board consists of 4 readout channels, which are connected with 37 pin D-sub connectors allowing up to 16 channels.

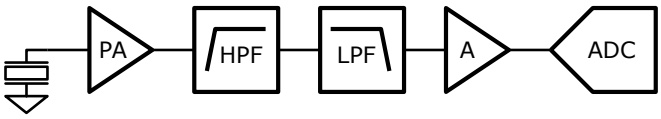

Fig. 1: System level of the readout circuit per channel.

The filtered and amplified analog signal is acquired by an ADC channel. In our case, two interconnected 16-bit 8-channel simultaneous sampling ADCs (USB-1608FS-Plus by Measurement Computing Corp) are employed. The ADCs are synchronized by setting one as a master, which will provide its clock to one or more slave ADCs, depending on the desired number of channels, via the SYNC port. The current configuration allows a simultaneous recording up to 16 or 8 channels at a maximum sampling rate of 50 or 100 kSamples/sec per channel respectively. The SYNC ports should be connected with the shortest possible wire to eliminate any delay due to parasitics. Simultaneous sampling was verified in the available bandwidth before the actual measurements.

Due to clinical safety concerns, the system is battery powered, which also reduces 60 Hz interference. Due to their high capacity and combined safety, NiMH batteries (Tenergy C size 1.2 V 5000 mAh) are selected and interconnected such as to achieve a ± 12 V supply. Hook and loop fasteners and Plug Connector are employed for stabilizing the position and connections respectively, and making the disassembly simple for charging the batteries. Low-dropout regulators (LDO) with programmable current are utilized to avoid a current excess in the start-up of the system. They are mounted on heat sinks to radiate the heat without damaging the LDOs, as illustrated in Fig. 2 (b).

All the parts of the system are piled up under 37 pin D-sub connectors and are enclosed in grounded aluminum boxes to reduce interference. The full setup is depicted in 2 (d). A special enclosure was designed to make it more patient-friendly and avoid any interaction of the user with the electronics.

B. Mechanical Module

One of the challenges of acquiring simultaneous recordings from the chest wall for quantitative acoustic investigations is the variation in signal intensity and frequency bandwidth associated with variations in contact pressure between the recording sensor and the body surface. In clinical auscultation, stethoscope pressure against the chest is empirically determined by the cardiologist.

In the current work, a specific module was implemented for ensuring firm attachment on the thoracic surface. The module was designed in Solidworks and 3D printed, as depicted in Fig. 2 (c). The module consists of two main parts: a fixed cylindrical holder, which is permanently attached to the vest, and a moving part, which includes the sensor and a spring. The spring is located between the bottom of the moving module and the sensor allowing the automatic adjustment. The firm placement of the sensor in a specific location provides the ability to conduct measurements in multiple positions, not only in supine position, which is the most common, but also in standing, sitting, or squat position.

C. Vest and Sensor Locations

A commercially available flotation vest was used to house the mechanical modules and the sensors. In order to generate an acoustic map, the microphones were allocated in a 4×3 grid on the chest and the upper abdominal muscles, as depicted in Fig. 2 (e). The dimensions are in cm. The placement of microphones directly over the sternum (prominent bone in the mid chest area) was avoided as the acoustic impedance of bone ($7.8 \cdot 10^6 kg \cdot s/m^3$) does not match the surrounding tissue ($1.48 \cdot 10^6 kg \cdot s/m^3$) and, hence, a high portion of the signal energy (around 40%) is reflected leading to a weaker signal on the body surface [12].

D. Software

MATLAB is used for data acquisition and post analysis. In addition to recording based on the set-up parameters, there is also an option for live monitoring, visual or auditory, of the microphones, which can be used to ensure that a signal of sufficient quality is acquired. Finally, an intuitive graphical user interface was created for post recording analysis, which allows data illustration or audition in a user friendly environment.

Fig. 2: System Compilation: (a) Readout Board, (b) LDO, (c) Mechanical Module, (d) Vest and Full system, (e) Sensors Location.

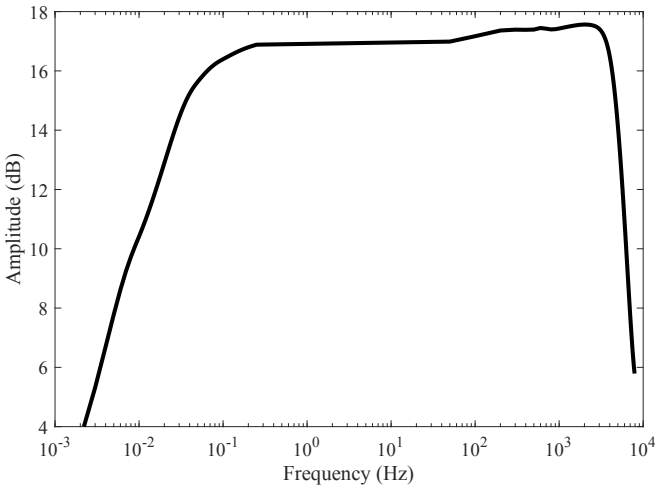

Fig. 3: Readout Channel Transfer Function

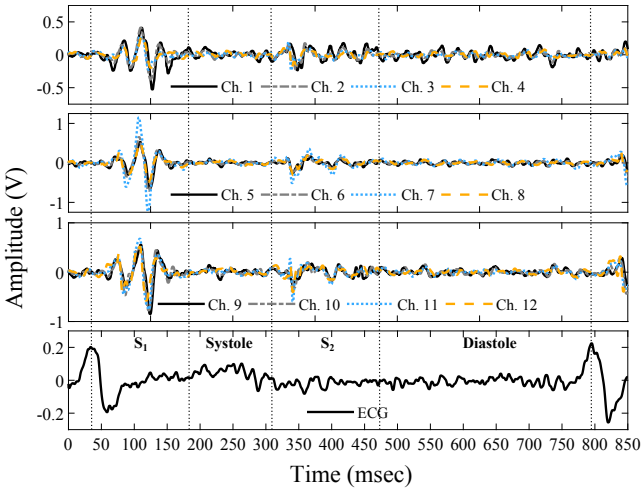

Fig. 4: Simultaneously recorded calibrated data for a cardiac cycle.

III. Results and Discussion

A. Readout Channels and Microphones calibration

Since the images are amplitude dependent, it should be ensured that there is no part of the setup that adds a systematic bias in the results. Thus, before proceeding to measurements, the readout channels and the microphones have to be characterized and any variations should be taken into consideration.

The frequency response of each channel was measured by employing a function generator (HP 33120A). Sinusoidal signals were fed via male jack cable to the channel input of each readout channel. The input signal ranged from 1 mHz to 8 kHz at a peak-to-peak voltage of 50 mV. The full procedure was automatized by MATLAB code, which was controlling the instrument via a National Instruments GPIB hardware (GPIB-USB-HS) and recording the channel response via an ADC. The system used the preamplifier, with gain set to 17 dB and the main amplification stage was used as a buffer, 0 dB. The median amplitude frequency response of the channels is depicted in Fig. 3 with a variation of ± 0.1 dB among the channels in the flat region (1 Hz - 1000 Hz).

Our system incorporates twelve Fukuda Denshi MA-250 sensors. This sensor model has shown capability of acquiring signal below 20 Hz and above 1000 Hz covering the range of the majority of heart sounds and murmurs (5-800 Hz).

Despite the similar responses of the channels, the microphones themselves require calibration in order to ensure that they provide a similar output in the same input. This is a more challenging case since the piezoelectric crystals could not provide the same intensity of signal even among exact same model sensors. In order to overcome this issue, a calibration coefficient is needed. The procedure to extract the parameter is by recording the response of each sensor to an artificial heart sound based on Morlet Wavelet. The sensors have similar waveform responses with different amplitude and, thus, the maximum absolute peak for each i sensor ($val(i)$) is selected. The formula to extract the calibration coefficients is described in Eq. 1:

$$coef(i) = \frac{mean(|val|)}{|val(i)|} \quad (1)$$

B. Acoustic Mapping Images

The data was recorded from a healthy male subject (27-year-old) in sitting position with breath-holding using the PCG sensors along with an ECG channel (BIOPAC ECG100C). The calibrated recordings for one cardiac cycle are superimposed in Fig. 4.

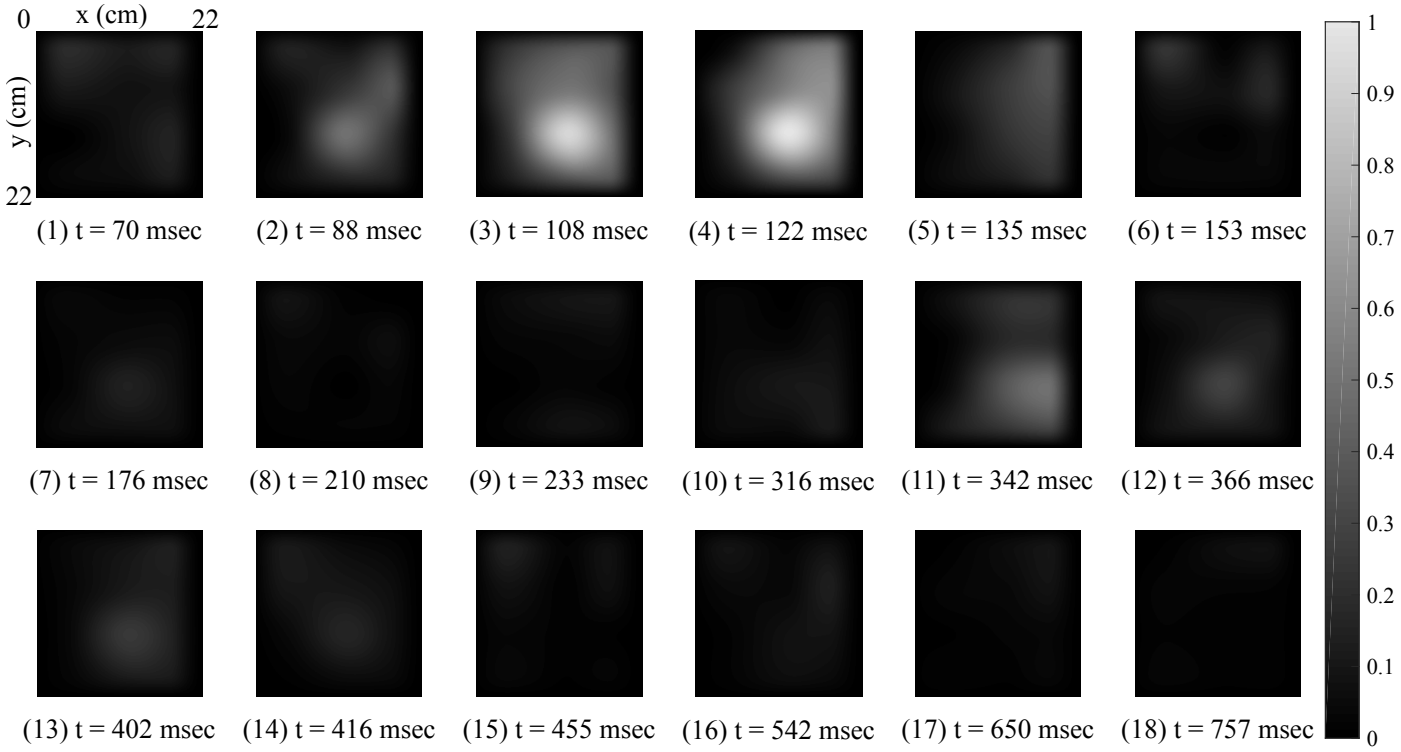

Fig. 5: Heart acoustic mapping captures for multiple moments during a cardiac cycle.

The cardiac acoustic mapping images use the normalized absolute value of the calibrated signal. Interpolation in between the recording sites is essential to achieve acoustic maps with smooth contours. A high resolution image (220×220) can be generated based on 4×3 array through Akima cubic interpolation, as illustrated in Fig. 5.

Each capture represents a chest wall area of $22cm \times 22cm$, as depicted in Fig. 2 (e). It mainly covers the surface anterior to the heart, displaying the received acoustic energy sequentially from early to late across a single cardiac cycle. The multiple acoustic captures show the propagation pattern of the heart sound on the thoracic surface. The subplots 5 (1), 5 (2-6) and 5 (7) show the pre, main and post S_1 sound respectively, which is due to the atrioventricular valves closure in the onset and the opening of semilunar valves at the end of the S_1. The captures 5 (8-9) represent the blood flow during systole from the ventricles to the aortic and pulmonary arteries. The subplots 5 (10-15) show the S_2 sound progress, consisting of sequential semilunar valve closures. Finally, diastole is illustrated in subplots 5 (16-18), where the blood flows into the right and left ventricle to complete the cardiac cycle.

IV. Conclusion

The current work provides a spatial and temporal representation of the propagation patterns of the heart function through PCG amplitude maps. A customized design of readout circuit along with the vest, which allows firm attachment to the thorax using a mechanical module for the sensor auto-adjustment, provide a system for reliable and time efficient operation. The system capabilities can be compared with previous efforts in Table I. The current setup will assist in conducting studies on the propagation patterns in healthy and unhealthy subjects and on source localization using beamforming techniques by taking advantage of the high sampling rate.

TABLE I: Comparison Table of Heart Acoustic Systems

Position	***Array Size***	***Simultaneity***	***Sampling Freq.***	***Ref.***
Supine	8×7	Yes	0.25 kHz	[7]
Supine	4×4	Yes	4 kHz	[8]
Sitting	2×4	Yes	10.24 kHz	[9]
Supine	8×8	No	3 kHz	[10]
Multiple	*4×3*	*Yes*	*50 or 100 kHz*	*CW*[a]

[a]Current Work.

References

[1] W. R. Thompson, "In defence of auscultation: a glorious future?" *Heart Asia*, vol. 9, no. 1, pp. 44–47, 2017.

[2] G. Kozmann and P. Kenedi, *Surface Acceleration Mapping: A New Method for Heart Sound Investigation*. Hungarian Acad. of Sciences, Central Research Inst. for Physics, 1976.

[3] K. Chihara, A. Kitajima, and Y. Sakurai, "Considerations on imaging method of diagnostic information of heart sounds," *IEICE Transactions (1976-1990)*, vol. 63, no. 9, pp. 670–671, 1980.

[4] M. Okada, "Chest wall maps of heart sounds and murmurs," *Computers and biomedical research*, vol. 15, no. 3, pp. 281–294, 1982.

[5] J. Verburg, "Transmission of vibrations of the heart to the chest wall," *Adv. Cardiovasc. Phys*, vol. 5, no. PART III, pp. 84–103, 1983.

[6] H. Vermarien, "Mapping and vector analysis of heart vibration data obtained by multisite phono-cardiography," *Adv. Cardiovasc. Phys*, vol. 6, pp. 133–185, 1989.

[7] M. Cozic, L.-G. Durand, and R. Guardo, "Development of a cardiac acoustic mapping system," *Medical and Biological Engineering and Computing*, vol. 36, no. 4, pp. 431–437, 1998.

[8] Y. Bahadirlar and H. Gulcur, "Cardiac passive acoustic localization: Cardiopal," *Turkish Journal of Electrical Engineering & Computer Sciences*, vol. 6, no. 3, pp. 243–260, 2000.

[9] M. Kompis, H. Pasterkamp, and G. R. Wodicka, "Acoustic imaging of the human chest," *Chest*, vol. 120, no. 4, pp. 1309–1321, 2001.

[10] F. Nogata, Y. Yokota, Y. Kawamura, H. Morita, and Y. Uno, "Visualization of heart motion by analysis of chest vibration," *Analysis of Biomedical Signals and Images*, vol. 20, pp. 11–16, 2010.

[11] A. G. Andreou, T. Abraham, W. R. Thompson, J. H. Seo, and R. Mittal, "Mapping the cardiac acousteome: An overview of technologies, tools and methods," in *Information Sciences and Systems (CISS), 2015 49th Annual Conference on*. IEEE, 2015, pp. 1–6.

[12] I. P. Herman, *Physics of the human body*. Springer, 2016.

BioCAS 2018

Biomedical Circuits and Systems Conference

Advanced Systems for Enhancing Human Health

Cleveland, Ohio, USA | October 17-19, 2018

The 2018 Biomedical Circuits and Systems Conference

hereby presents the

3rd Best Paper Award

to

Christos Sapsanis, Nathaniel Welsh, Michael Pozin, Guillaume Garreau, Gaspar Tognetti, Hani Bakhshaee, Philippe O. Pouliquen, Rajat Mittal, William R. Thompson, andAndreas G. Andreou

for the paper entitled

StethoVest: A simultaneous multichannel wearable system for cardiac acoustic mapping

Timothy Constandinou	*Maysam Ghovanloo*	*Jun Ohta*
Technical Program Chair	*Technical Program Chair*	*Technical Program Chair*
BioCAS 2018	*BioCAS 2018*	*BioCAS 2018*